Separation Science and Technology
Publication details, including instructions for authors and subscription information:
http://www.informaworld.com/smpp/title~content=t713708471

Photodegradation of Natural Organic Matter in Water with UV Irradiation at 185 and 254 nm: Importance of Hydrodynamic Conditions on the Decomposition Rate

S. Dobrović[a]; H. Juretić[a]; N. Ružinski[a]
[a] Faculty of Mechanical Engineering and Naval Architecture, University of Zagreb, Zagreb, Croatia

To cite this Article Dobrović, S. , Juretić, H. and Ružinski, N.(2007) 'Photodegradation of Natural Organic Matter in Water with UV Irradiation at 185 and 254 nm: Importance of Hydrodynamic Conditions on the Decomposition Rate', Separation Science and Technology, 42: 7, 1421 — 1432

To link to this Article: DOI: 10.1080/01496390701289849

URL: http://dx.doi.org/10.1080/01496390701289849

Separation Science and Technology, 42: 1421–1432, 2007

ISSN 0149-6395 print/1520-5754 online
DOI: 10.1080/01496390701289849

Photodegradation of Natural Organic Matter in Water with UV Irradiation at 185 and 254 nm: Importance of Hydrodynamic Conditions on the Decomposition Rate

S. Dobrović, H. Juretić, and N. Ružinski
University of Zagreb, Faculty of Mechanical Engineering and Naval Architecture, Zagreb, Croatia

Abstract: The kinetic investigation of photodegradation of the natural organic matter (NOM) in natural lake water was conducted using two low-pressure mercury lamps of the same nominal power: a) with suprasil quartz envelope emitting at both wavelengths −254 nm and 185 nm (hereafter VUV); b) with standard quartz envelope emitting only at 254 nm (hereafter UV). In comparison to the UV process, the addition of 185 nm irradiation (VUV process) increased the degradation rate ten-fold overall at lower and seventeen-fold at higher Reynolds numbers, respectively. The hydrodynamic characteristics of the photoreactor are of crucial importance for total energy efficiency for VUV processes.

Keywords: Photodegradation, hydrodynamic conditions, degradation rate, Reynolds number, VUV, UV

INTRODUCTION

Natural organic matter (NOM) is a mixture of poorly defined organic compounds that are normally present in ground and surface waters, and their residuals in drinking water are considered to pose a significant problem (1). Interactions of NOM with chlorine based disinfection agents

Received 2 November 2006, Accepted 20 February 2007

Address correspondence to S. Dobrović, University of ZagrebFaculty of Mechanical Engineering and Naval Architecture, Ivana Lučića 5, Zagreb, Croatia. E-mail: slaven.dobrovic@fsb.hr

lead to the formation of carcinogenic and mutagenic disinfection by-products. Other problems associated with the presence of NOM in water include complexation with heavy metal ions, influence on organoleptic quality of water, and the fact that NOM acts as an energetic and nutritive substrate for microbial growth within distribution systems (2).

Among the processes for the NOM separation from (drinking) water, a marked position has advanced oxidation processes (AOPs). NOM separation employing (AOPs) is mainly based on the efficient generation of highly reactive, powerful oxidant hydroxyl radical ($HO^{\bullet}$), which cause partial oxidation or total mineralization of organic matter (3). The majority of AOPs are based on photolysis of added oxidants—O_3 and H_2O_2 by UV light that results in the production of strong oxidizing species like $HO^{\bullet}$. However, vacuum-ultraviolet AOPs are mainly based on photochemically initiated homolysis of water that results in the generation of hydroxyl radicals and hydrogen atoms. As sources of VUV irradiation, a xenon excimer lamp with emission maximum at $\lambda = 172$ nm, and a standard low-pressure mercury lamp with part of its emission spectra at $\lambda = 185$ nm can be used. The limitation of these processes arises from short lifetimes of generated radicals and a relatively high absorption cross section of water in the VUV part of spectra, leading to the formation of better irradiated areas of a reactor rich in radicals but depleted organics. Short-living $HO^{\bullet}$ and $H^{\bullet}$ cannot diffuse far outside the irradiated area, and all the reactions are taking place within the restricted volume. This leads to extreme heterogeneity between the irradiated and non-irradiated volume and the overall efficiency of the oxidation process is limited. In order to improve the efficiency of the VUV based advanced oxidation process some improvements have been made. Increased rate of mineralization has been achieved with injection of molecular oxygen within the zone of thermal and radical reactions (4). Another way to improve the efficiency was done by conducting two simultaneous but separate photochemical reactions with a single light source:

i. photochemical generation of ozone by irradiating oxygen in the gas phase and
ii. photolysis of the aqueous reaction system.

The gas stream containing the generated ozone is sparged into the reaction system, resulting in an increase of overall oxidative degradation efficiency (5). Although there are some reports on the contribution of irradiation at $\lambda = 185$ nm to the degradation process, to our knowledge there is little data about achievable improvement of the efficiency by changing the hydrodynamic conditions in the system, especially with natural water samples (4, 6, 7). To characterize the hydrodynamic state within the system of the UV reactor, dimensionless Reynolds number was used. There are several reports relating to mass transfer controlled processes observed at particular Reynolds numbers conditions (8–13), but the results of this study bring new insights with regard to the importance of hydrodynamic conditions of photodegradation processes based on both UV and VUV irradiation on its decomposition rate or on its overall efficiency.

METHODS

Experiments were done with natural water with humic character from lake Njivice on Island Krk, Croatia, that has been used for drinking water distribution after treatment on the nearby plant. Samples were collected from a raw water pipeline of the facility, kept in PC polymer containers (capacity 30 L) in the dark at 4°C for no longer than 4 days. The quality of water was monitored by spectroscopic analysis prior to each set of experiments. The change of initial UV absorbance at 254 nm of stored water during its experimental period (4 days) was always within 2%. The UV-VIS spectra of the raw water is given by the Fig. 1.

Quality of the Lake Water

Absorbance at 254 nm in range of 0.114–0.135 cm^{-1}, TOC content in range of 4.56–5.1 mg l^{-1}, measured as NPOC, nonpurgeable organic carbon, after acidification to pH 2.5, total hardness 198–290 ppm $CaCO_3$, alkalinity 166–234 ppm $CaCO_3$, nitrate 0.00–0.44 mgN/l. Kinetics were performed spectrophotometrically (Hewlett Packard, model 8453) by following the decrease in the 254 nm absorbance of the humic substances irradiated. Kinetic data of the degradation processes was processed using standard

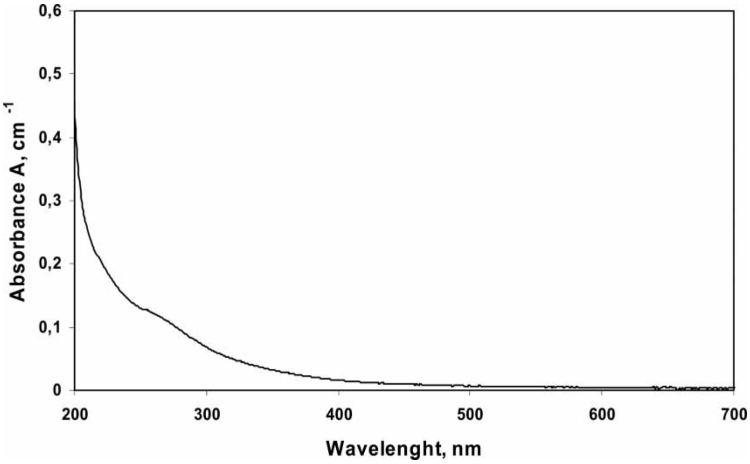

Figure 1. UV-VIS spectra of raw lake water rich in NOM.

non-linear regression analysis (with Statistical Analysis software, StatSoft Inc.) based on pseudo first order kinetics formulation. The content of NOM was measured by means of $KMnO_4$ oxidation (hereafter COD). For the COD measurements, 4 ml of sample was mixed with 4 ml of standard $KMnO_4$ solution (0.712×10^{-3} mol l^{-1}) and one drop of sulphuric acid (98% by weight) is added (adopted from (14)). The Mixture was heated for two hours at 80°C in a COD reactor (by Hach Company, U.S.A.). The absorbance of residual permanganate was measured at $\lambda = 522$ nm ($\varepsilon_{MnO_4^-} = 2370$ l mol^{-1} cm^{-1}) by a spectrophotometer (Hewlett Packard 8453). Prior to measurements of absorbance, the sample was filtered on a membrane filter with pore diameter 0.45 μm (type ME 25, by Schleicher and Schuell, Germany). All the chemicals used were of analytical grade purity (ALDRICH or FLUKA). The pH was determined using WTW pH – meter 540 GLP equipped with combined glass WTW SenTix 97T electrode and usually was in the range 7.70 – 7.90.

The reactor system used in this study is presented in Fig. 2. The net volume of the tubular photoreactor was 606 ml, with a total length of 790 mm, and with length of light path through water of 7.5 mm (from quartz envelope to glassy wall of the reactor). The UV lamp was centrally placed inside of the suprasil quality quartz tube with an external diameter of 25 mm. Construction materials of the reactor are quartz, glass, and stainless steel (AISI 316L). Besides chemically highly resistant peristaltic tubes, all other tubing was made of PTFE. For both types of low-pressure

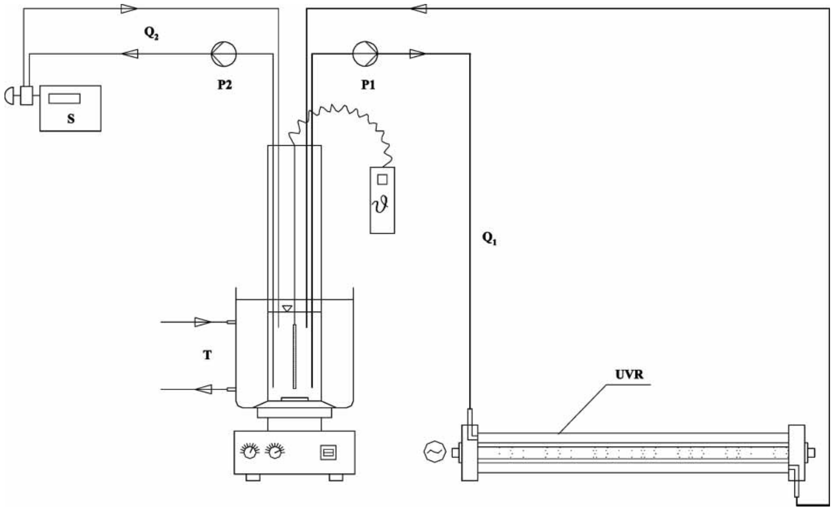

Figure 2. Schematic drawing of the photoreactor system and experimental set up. UVR—photoreactor, P1 peristaltic pump 1 for flow rate $Q_1 = 10\text{-}85$ ml/s, P2 peristaltic pump 2 for flow rate $Q_2 = 6$ ml/min, S—UV/VIS spectrophotometer with flow- through quartz cell, T—thermostating bath.

mercury lamps that were used, stated total watts of ultraviolet output was 13.8 W with corresponding electric power of 39 W (by Wedeco Ideal Horizons, USA). According to the manufacturer, the UV output for the VUV lamp at 254 and 185 nm are >120 μWs/cm^2 and >6 μWs/cm^2 respectively. UV lamp emits only at 254 nm with intensity >120 μWs/cm^2. The temperature in the photoreactor during the photodecomposition process was kept constant by means of a thermostat, and was monitored online by a TESTO 110 immersion probe thermometer.

Since the photoreactor consists of two coaxial cylindrical tubes with a low-pressure mercury lamp centrally placed in the axis (Fig. 3), the Reynolds number (Re) calculation was based on the hydraulic diameter of the photoreactor as follows.

$$\mathrm{Re} = \frac{vl}{\nu} \tag{1}$$

v−mean fluid velocity, m/s

l−characteristic length, here hydraulic diameter D_h, m

ν−kinematic fluid viscosity, m^2/s

$$l = D_h = \frac{4F}{O} = \frac{4\pi/4(D^2 - d^2)}{\pi(D + d)} = D - d \tag{2}$$

F−area section of the duct, m^2

O−wetted perimeter of the duct, m

D−internal diameter of glass wall of reactor

d−external diameter of quartz envelope of UV/VUV lamp.

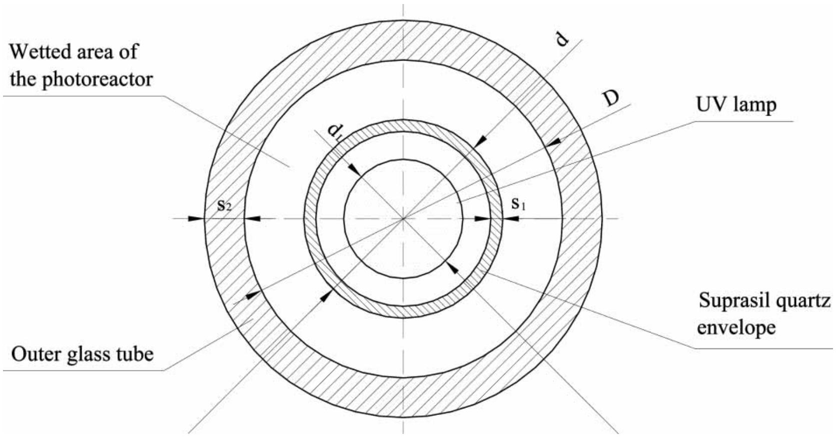

Figure 3. Cross-sectional view of the photoreactor. D = 40 mm, d = 25 mm, d_L = 19 mm, s_1 = 1.5 mm, s_2 = 5 mm.

RESULTS AND DISCUSSION

Kinetic Investigation

As can be partly seen in Fig. 4, the photoinduced decomposition of NOM under irradiation of VUV light follows very well the pseudo-first order kinetics for at least four half-time lives. Kinetics were performed spectrophotometrically, continuously monitoring the absorbance at 254 nm. The decomposition process of NOM under irradiation of solely UV is much slower but again could be simulated by the following pseudo first-order kinetics during the observed two half-times. This is in accordance with other water reports (15), on the kinetics of the photoinduced degradation of natural humic substances. Data explaining the photodegradation process presented in Fig. 4 is given in Table 1.

The total reduction of the NOM content is much lower than the reduction of absorbance at 254 nm at the observed experimental time, but significantly dependent on whether the 185 nm photons were involved. But the VUV processes involving strong 185 nm photons reduction NOM content was 42 to 46%, compared to the negligible mineralization by the UV processes at the observed experimental time. This response to UV irradiation has been reported and is due to the specific chemical change taking place during the photodegradation of NOM. The photodegradation processes of complex natural organic matter, start with the formation of lower molecular weight fragments (mainly organic acids like formic, acetic, succinic, oxalic, glyoxalic, and many others) and then proceeds with the final mineralization

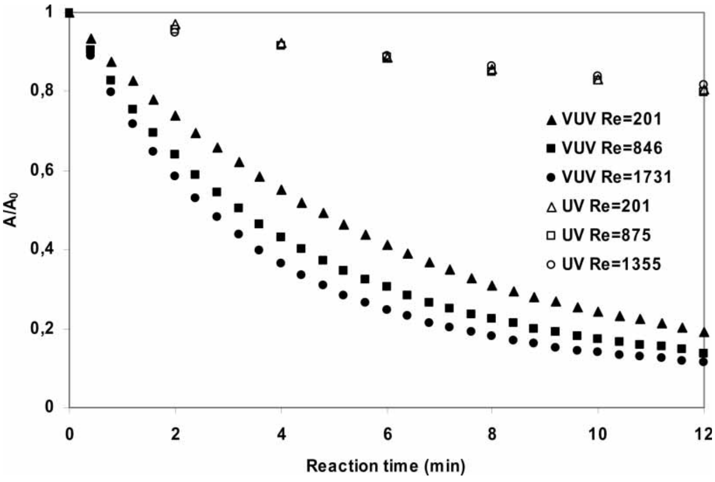

Figure 4. Photodegradation of NOM under VUV and UV irradiation at different Re numbers. A absorbance at 254 nm.

Table 1. Kinetic data of particular VUV and UV process presented in Fig. 4

Process	Reynolds number (Re)	Reaction constant[a] (k, min^{-1})	Half-time,[a,b] (min)	Absorbance reduction[c] (%)	COD reduction[c]	Temperature (°C)
VUV-254/185 nm	201	6.744×10^{-2}	4.15	80.7	45%	21.5
VUV-254/185 nm	846	9.87×10^{-2}	2.84	86.3	42%	21.8
VUV-254/185 nm	1371	12.150×10^{-2}	2.31	88.5	46%	22.2
UV-254 nm	201	6.960 x 10^{-3}	40.3	18.5	~0	21.5
UV-254 nm	875	6.720×10^{-3}	41.3	20.4	~0	22.0
UV-254 nm	1355	6.780×10^{-3}	41.7	19.5	~0	22.2

[a] Pseudo-first order kinetics based on decrease in the 254 nm absorbance of irradiated water.

[b] Reaction time given in net time considering the volume ratio of irradiated and total processed water. Ratio is 0.404.

[c] Absorbance and COD reduction after the 12 net minutes of photodegradation.

to CO_2, water, and salts (16–18). Anyhow, the initial and it seems the unavoidable phase of photodegradation of NOM is defragmentation of the complex NOM structure that could be properly monitored by UV absorption, as it was done within this work. Besides, these organic products, compared to the original organic substance, are much more biodegradable, so they could be simply removed by subsequent filtration. This means that in order to optimize the possible water treatment process considering the specific energy consumption, the photoinduced degradation of NOM and some other less energy demanding processes such as filtration could be properly balanced.

Comparison between UV and VUV

When compared to the UV based processes, VUV photodegradation processes are ten times faster at lower and seventeen times at higher Reynolds numbers, respectively. Thus, the contribution of irradiation at $\lambda = 185$ nm is very significant, and efficiency of its use is greatly dependent on the hydrodynamic properties of the flow within the reactor. The same change of flow intensity–from Re $\approx$ 200 to Re $\approx$ 860 caused the increase of the degradation rate by 33% at VUV and negligible 1% at UV processes. Further increase of the Re number (from 200 to 1330) speed up VUV process by 40% and UV process by just 3%.

The tremendous differences in the rates of degradation between VUV and UV processes are a consequence of the in situ formation of radical oxidants via the photolysis of water at 185 nm and subsequent reaction with NOM.

This contribution of 185 nm photons by the photolysis of water and generation of hydroxyl radical and other oxidants is according to the following principal reactions:

$$H_2O \xrightarrow{UV_{185nm}} H^\bullet + HO^\bullet$$

$$2HO^\bullet \longrightarrow H_2O_2$$

$$H^\bullet + O_2 \longrightarrow HO_2^\bullet$$

These generated radical oxidants are extremely short-lived and if not used in reaction with NOM, they undergo self-destruction or their strong oxidation potential is inhibited by the alkalinity of water (3, 19).

The penetration depth of VUV light into water is very short due to the high absorption coefficient of water being approximately $a = 1.8\,cm^{-1}$ at $\lambda = 185$ nm (20). That means that only 4% of UV light arrived at the outer glass wall of the UV reactor through 7.5 mm of water. Considering the fact that the absorption results in the generation of short-lived radical oxidant species, there is resultant profile concentration of radicals that has a logarithmic shape. The cross section profile of the NOM concentration in the UV reactor could be considered as constant, although at slower flow rates at the end of the rector, a decrease of the NOM content in the radical rich zone could be expected. Thus, a cross section profile of the NOM concentration gains a reverse shape of that of the radicals. That leads to enhanced heterogeneity

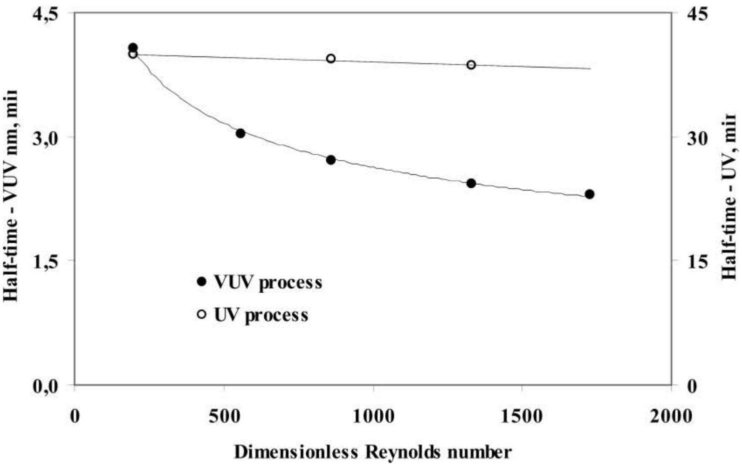

Figure 5. Kinetic data—photodegradation of NOM under VUV and UV irradiation at different Re numbers.

within the photochemical reactor and limited overall efficiency of the oxidation process.

Intensified flow rate, expressed by an increase of Reynolds number, although still in a laminar flow regime, allows better mixing and a more effective mass transfer of the reactants is achieved.

As can be seen in Fig. 5 and Table 2, the photodegradation process based on the UV irradiation at $\lambda = 254$ nm (UV process) has a completely different

Table 2. Kinetic data of VUV and UV processes presented in Fig. 5

Process	Reynolds number (Re)	Half-time,[a,b,c] (min)	Standard deviation (min)	Temperature (°C)
VUV-254/185 nm	~200	4.07	0.14	21.5
VUV-254/185 nm	~560	3.04	0.14	21.6
VUV-254/185 nm	~860	2.71	0.18	22.0
VUV-254/185 nm	~1330	2.43	0.12	22.1
VUV-254/185 nm	~1730	2.30	0.11	22.2
UV-254 nm	~200	39.91	0.49	21.5
UV-254 nm	~860	39.34	2.20	22.0
UV-254 nm	~1330	38.54	4.47	22.3

[a] Pseudo-first order kinetics based on decrease in the 254 nm absorbance of irradiated water.

[b] Reaction time given in net time considering the volume ratio of irradiated and total processed water. Ratio is 0.404.

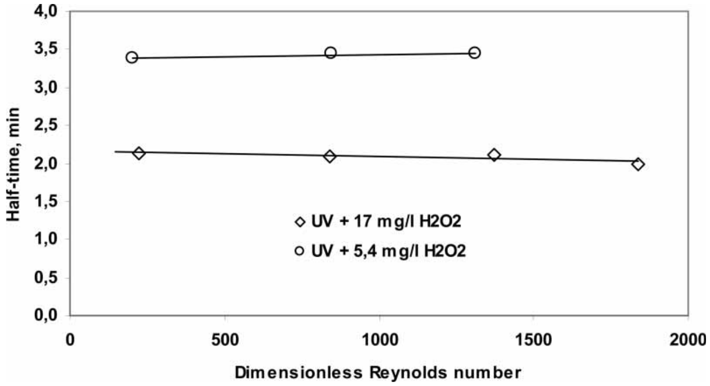

Figure 6. Kinetic data—photodegradation of NOM under UV irradiation and H_2O_2 at different Re numbers.

response to hydrodynamic change. The only absorbing compound is NOM, and since the absorbance at 254 nm was 0.12 cm^{-1} at the beginning of the process, more than 80% of 254 nm irradiation reached the outer glass wall of the UV reactor through the 7.5 mm thick layer of circulating water. Thus the intensity of irradiation is quite uniform and the only way to improve the process is to enlarge the reactor diameter and consequently its volume.

When combining UV irradiation with H_2O_2, another advanced oxidation process (AOP) is obtained, and hydroxyl radicals are produced. This time generated radicals are dispersed equally, because, the first reactant, H_2O_2, is well-mixed and homogeneously distributed in water and the second reactant, 254 nm photon is well-transmitted through the reaction mixture.

Table 3. Kinetic data of particular UV-H_2O_2 process presented in Fig. 6

Process	Reynolds number (Re)	H_2O_2 dose,[c] (mg/l)	Reaction constant[a] (k, $min^{-1)}$	Half-time[a,b] (min)	Temperature (°C)
UV-H_2O_2	201	5.4	8.274×10^{-2}	3.39	21.5
UV-H_2O_2	846	5.4	8.148×10^{-2}	3.44	21.5
UV-H_2O_2	1309	5.4	8.124×10^{-2}	3.45	21.5
UV-H_2O_2	224	17.0	13.1×10^{-2}	2.13	21.5
UV-H_2O_2	842	17.0	13.4×10^{-2}	2.09	21.7
UV-H_2O_2	1372	17.0	13.25×10^{-2}	2.12	22.8
UV-H_2O_2	1836	17.0	14.07×10^{-2}	1.99	23.2

[a] Pseudo-first order kinetics based on decrease in the 254 nm absorbance of irradiated water.

[b] Reaction time given in net time considering the volume ratio of irradiated and total processed water. Ratio is 0.404.

The only question is whether the radical's short lifetime limitation could be influenced by hydrodynamic properties of flow within the reactor. Experiments conducted with two dosages of H_2O_2 at different flow intensities expressed with the Re number are summarized in Fig. 6 and Table 3. It is obvious that the degradation rate of NOM in UV—the H_2O_2 processes are not dependent on the flow intensity, therefore the mass transfer is not a limitation factor as it is at VUV processes.

CONCLUSION

The photodegradation process with low-pressure mercury lamp with standard quartz which emits UV irradiation at $\lambda = 254$ nm (UV process), is not influenced with the hydrodynamic properties of the process at all. The UV process at $\lambda = 254$ nm without the addition of H_2O_2 is primarily based on the direct photolysis of the complex structure of the natural organic matter and mixing and mass transfer is not a limiting factor.

On the contrary, the degradation process that includes irradiation at $\lambda = 185$ nm (VUV process) is based on radicals generated by the photolysis of water. Due to the short lifetime of generated radicals and a relatively high absorption coefficient of water at $\lambda = 185$ nm, the logarithmic profile of radicals is formed. Thus, different zones within the photochemical reactor are formed—zone close to the UV source rich in the radicals but depleted organics, and zone distant from the UV source, rich in NOM but poor in generated radicals. Therefore the reactants are not balanced on both sides, and a hydrodynamic change could enhance mass transfer and therefore improve the degradation rate as it is shown in this paper.

The UV-H_2O_2 process is not dependent on the hydrodynamic properties within the UV reactor at both dosages of H_2O_2. The conclusion is that the UV-H_2O_2 process is not mass transfer controlled even considering an extremely short lifetime of the radical species.

ACKNOWLEDGEMENTS

Financial support from the Ministry of Science and Technology of the Republic of Croatia (scientific project 0120026) is acknowledged.

REFERENCES

1. vanLoon, G.W. and Duffy, S.J. (2000) *Environmental Chemisty*, 1st Ed; Oxford University Press: Oxford, New York.
2. Pomes, M.L. et al. (1999) DBP formation potential of aquatic humic substances. *Journal AWWA*, 91 (3): 103.

3. Legrini, O., Oliveros, E., and Braun, A.M. (1993) Photochemical processes for water treatment. *Chemical Reviews*, 93: 67.
4. Oppenländer, T. et al. (2005) Improved vacuum-UV (VUV)-initiated photomineralization of organic compounds in water with a xenon excimer flow-through photoreactor (Xe_2^* lamp, 172 nm) containing an axially centered ceramic oxygenator. *Chemosphere*, 60: 302.
5. Hashem, T.M., Zirlewagen, M., and Braun, A.M. (1997) Simultaneous photochemical generation of ozone in the gas phase and photolysis of aqueous reaction systems using one VUV light source. *Water Science and Technology*, 35: 41.
6. Han, W. et al. (2004) Photocatalytic degradation of phenols in aqueous solution under irradiation of 254 and 185 nm UV light. *Catalysis Today*, 90: 319.
7. Zhang, Z., Anderson, W.A., and Moo-Young, M. (2003) Modeling of corrugated plate photocatalytic reactors and experimental validation. *Chemical Engineering Science*, 58: 911.
8. Balanosky, E., Herrera, F., Lopez, A., and Kiwi, J. (1999) Oxidative degradation of textile waste water. Modeling reactor performance. *Water Research*, 34 (2): 582.
9. Koutchma, T., Keller, S., Chirtel, S., and Parisi, B. (2004) Ultraviolet disinfection of juice products in laminar and turbulent flow reactors. *Innovative Food Science & Emerging Technologies*, 5: 179.
10. Lin, H.F., Ravikrishna, R., and Valsaraj, K.T. (2002) Reusable adsorbents for dilute solution separation. 6. Batch and continuous reactors for the adsorption and degradation of 1,2-dichlorobenzene from dilute wastewater streams using titania as a photocatalyst. *Separation and Purification Technology*, 28: 87.
11. Tabrizi, G.B. and Mehrvar, M. (2006) Pilot-plant study for the photochemical treatment of aqueous linear alkylbenzene sulfonate. *Separation and Purification Technology*, 49: 115.
12. Taghipour, F. and Sozzi, A. (2005) Modeling and design of ultraviolet reactors for disinfection by-product precursor removal. *Desalination*, 176: 71.
13. Daneshvar, N. et al. (2005) Photooxidative degradation of Acid Red 27 in a tubular continuous-flow photoreactor: influence of operational parameters and mineralization products. *Journal of Hazardous Materials*, 118: 155.
14. Andreozzi, R. et al. (1999) Advanced oxidation processes for the treatment of mineral oil-contaminated wastewaters. *Water Research*, 34 (2): 620.
15. Uyguner, C.S. and Bekbolet, M. (2005) Evaluation of humic acid photocatalytic degradation by UV–vis and fluorescence spectroscopy. *Catalysis Today*, 101: 267.
16. Corin, N., Backlund, P., and Kulovaara, M. (1996) Degradation products formed during UV-irradiation of humic waters. *Chemosphere*, 33 (2): 245.
17. Allard, B., et al. (1994) Degradation of humic substances by UV irradiation. *Environmental International*, 20 (1): 97.
18. Backlund, P. (1992) Degradation of aquatic humic material by ultraviolet light. *Chemosphere*, 25 (12): 1869.
19. Gonzalez, M.G., Oliveros, E., Wörner, M., and Braun, A.M. (2004) Vacuum-ultraviolet photolysis of aqueous reaction systems. *Journal of Photochemistry and Photobiology C: Photochemistry Reviews*, 5: 225.
20. Weeks, J.L., Meaburn, G.M.A.C., and Gordon, S. (1963) Absorption coefficients of liquid water and aqueous solution in the far ultraviolet. *Radiation Research*, 19: 559.